Journal of Radiation and Nuclear Applications
*An International Journal*

http://dx.doi.org/10.18576/jrna/080202

# Evaluation the Image Registry for PET -CT and Image Artifacts and Correction for Radiation Treatment Planning for Cancer Patients (Lung Cancer)

*A.F. Asaad* [1], *H. M. Abu zeid*[2], *H. A. Ashry*[3], *Kh. M. Elshahat*[4] *H. William*[5], *A. GabAllah*[6]

[1] Department of Radiotherapy, IMC, Cairo, Egypt.
[2]Department of Physics, Faculty of Women for Art, Sciences and Education -Ain shams University- Cairo -Egypt
[3]EAEA – Cairo- Egypt.
[4]Clinical Oncology Dept.- Faculty of Medicine – Al-Azhar University- Cairo- Egypt.
[5]Radiotherapy department, -Ahmed Maher educational Hospital.
[6]Department of Clinical Oncology – Faculty of Medicine – Ain shams university -Cairo-Egypt.

Received: 28 Feb. 2023, Revised: 12 Mar. 2023, Accepted: 22 Mar. 2223.
Published online: 1 May 2023.

**Abstract:** Propels in innovation have permitted very exact control of radiation portion conveyance and limitation inside a patient. The capacity to confidently outline target growth limits, but has fallen behind. F-FDG PET/CT, with its capacity to recognize metabolically dynamic tumor from normal tissue, may give a halfway answer to this issue. Here we survey the momentum uses of 18F-FDG PET/CT in an assortment of sickness locales, including non-little cell cellular breakdown in the lung's cancer patients. The utilization of $^{18}$F-FDG PET/CT to help with arranging radiotherapy and the related benefits and challenges. **Results**: in the review deformity, an exact patient-explicit registration model was worked with an objective enlistment blunder of 3.2±1.7 mm**. Conclusion**: Image misshapen because of the impact of gravity was effectively displayed by the limited component strategies

**Keywords:** Lung cancer patient- PET-CT- Registration.

## 1 Introduction

Modern radiotherapy makes it possible to control more accurately where the radiation dose is distributed within the patient, to irradiate tumor tissue (and risk areas) from locoregional metastases, and at the same time save it close to normal tissue.

. Intensity-modulated radiotherapy (IMRT)and VMAT are the most advanced technology available for cancer treatment [1-3]. IMRT and VMAT effectively adjusts dose distribution using many possible degrees of freedom with spatial intensity modulation than more traditional 3-dimensional compliant radiotherapy methods. With IMRT and VMAT in lung cases, for example, a radiation oncologist can provide concave dose distributions that treat large areas of the lung that wrap around the spinal cord and can limit the spinal cord itself to a relatively low intake, thereby minimizing cord damage. [2]. It is also possible to have spatially limited dose distributions that treat lung tumors while rescuing normal lung and heart tumors, while brain nerves and optic chiasma-like tumors lung in the rescue of the adjacent heart and spinal cord [3-7] Many IMRT implementations are more available than commercial products [8] and improved techniques such as volume arches, treatments that treat several continuous gantry sweep tumors around the patient are under development. in one or more arcs [9,10]. These dose improvements accompany new ways of locating the patient's tumor and normal tissues during treatment. Although traditional methods rely on n-based skin laser scaling augmented by periodic orthogonal X-rays, modern radiotherapy clinics may use stereoscopic kilovoltage radiography as integrated CT guidance that allows the patient to be accurately tuned to the treatment beam [8, 11, 12].

Monitoring of patient position and dynamic changes during treatment is also possible using various currently available technologies [13 -15]. This general paradigm of active use of imaging during treatment is called image-guided radiotherapy. This makes it possible to define about half of the remaining structural localization error as the goal of the treatment plan process, as determined by repeated imaging [16]. The extent to which localization error can be minimized depends on the site being treated, with intracranial tumors being the best and worst case. is one

*Corresponding author e-mail: aymanfathy1011@yahoo.com

that has a lot of movement and is difficult to see as a gastrointestinal site.

***- Contouring: -***

-The following organ and risk structures (OARs) are described: Lung, Heart modification (manual lung volume based on lung on cone-beam CT mages of the first three RT fractions), spinal cord. Gross tumor volume (GTV) contamination in the lung NSLC should be performed by knowledgeable readers, taking into account all available information. PET-based GTV (GTV-PET) contouring should be performed according to two recommendations: (i) for PET Scaling Manual - SUVmin-max: 0 - 10 for 18FDG. Any record higher than the neighboring background should be considered LCa [18]. (ii) Semi-automatic delineation, in which the SUVmax value must be calculated for each injury, and 30% (range: 20-40%) of these SUVmax values must be used as the threshold value according to previous studies [18]. Additional GTV-PET-based trackers should be tuned to each experience center. A convolutional neural network can be used to define GTV [51], but contours are often re-examined by experienced readers. In the case of ADT management, the GTV-CT for planning should be tuned during image processing before the ADT. Eventually, all GTVs are merged into one GTV volume.

Despite all these technologies, the crucial problem of accurately controlling the delivery of the radiation dose remains to determine which area of tissue is needed.
purpose. This aspect of radiotherapy design is perhaps the most challenging. Interobserver innovation with CT scanning has been well evaluated and documented for a variety of common diseases, including lung and head, and neck cancer [18], and due to the difficulty of determining the exact limit. in the tumor and for professional observers with the most advanced CT protocols.

-Without proper separation of the tumor area, first control of the dose distribution may not provide greater control over the tumor. In this regard, a PET scan with an $^{18}$F-FDG radio indicator may be most useful. In many common cancers, PET with $^{18}$F-FDG or in combination with CT has with $^{18}$F-FDG or in combination with CT has greater sensitivity and specificity for disease analysis than CT or MRI alone [18]. Due to its ability to identify metabolically active diseases, F-FDG PET / CT can provide important supplemental information on the treatment plan proposal.

Figure 1 shows an example of a patient with lung cancer. In this case, the radiation oncologist delimits the tumor area based on CT (yellow) and the nuclear medicine physician draws the tumor based on 18F-FDG PET / CT) blue). The addition of 18F-FDG PET / CT provided clear evidence of disease reaching about 2 cm below the CT limit alone.

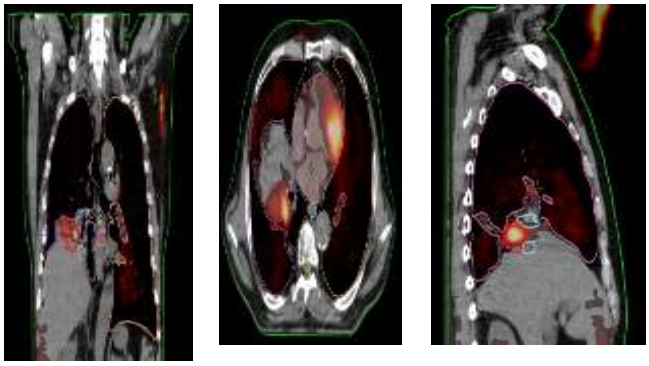

**Fig.1:** Lung cancer in different Views for CT fusion with PET/CT.

Although there is a slight registration error between PET and CT due to respiratory movement this separation between the two areas showed a real difference between the apparent tumor locations in the 182 studies. This article focuses on the usage F-FDG PET / CT to improve the target definition of IMRT and VMAT planning. Of course, this is just one way 18 F-FDG PET is used to manage the care of cancer patients. Other uses of 18 F-FDG PET include better disease staging determining whether curative radiotherapy is appropriate [12-14) and measuring the response to treatment for further management applied to different areas of the disease [15-18]. While most cancers are $^{18}$F-FDG - avid, others - such as mucinous cancers of the colon, stomach, and other areas - may be less common. Areas for treatment should therefore be acquired with knowledge of untreated tumor stimulation for 18F-FDG. This review focuses on disease areas where $^{18}$F-FDG PET / CT tumors are currently widely used for IMRT and VMAT planning. We will start by discussing the many problems with the physical image that affect almost every use of this technology.

## 2 Physical Problems

-Tumor boundary separation the main benefit of $^{18}$F-FDG PET in radiotherapy planning is its potential to improve tumor boundary separation. $^{18}$F-FDG PET can provide a better indication of the true extent of the disease and can also reduce inter-server variability, making the number of treatments more standardized by a wide range of physicians and clients. various writers [17-18]. The need for robust separation of tumor boundaries has become more important in treatment modalities that deliver a single dose of relatively small, high-dose fractions (10-30 Gy), such as stereotactic body radiotherapy., made to treat the lungs. and panko's and other sites. In high-dose regimens, small margins around the tumor are used to maintain normal surrounding tissue. However, when using small margins, there is not much room for error. If the actual tumor is not properly tuned, it will fall out of the high dose volume. In the standard fractionation approach (e.g. 30 fractions of 2 Gy each), a large margin of approximately 1 cm is used

around the tumor. The standard definition (International Commission on Radiation Units and Measurements, ICRU50) consists of gross tumor volume (GTV), which is the radiologically acceptable tumor size, extended to the clinical target volume to account for microscopic expansion, and finally to the planned target PTV volume) with various physical uncertainties, such as movement during treatment or daily tissue repositioning. In the high dose scheme, the localization is strict and uses a range between GTV and PTV of only a few millimeters; for example, 2-3 mm is used for stereotactic body radiotherapy in the pancreas or 5 mm axially for the lungs. With such a strict localization, one must be sure of the separation accuracy, and F-FDG PET / CT can play an important role in this. Great attention must also be paid to the technical quality of the PET / CT scan to minimize possible erroneous registration between PET and CT images, which are acquired sequentially and not simultaneously.

[1] One aspect is respiratory function. When aligning tumor boundaries with 18F-FDG PET, severalphysical imaging issues are likely to affect all treatment sites (4). The first is the depreciation method itself. Two challenges need to be overcome here. The first is related to the spatial resolution of the PET image, which, as used in clinical practice, is 7-9 mm in many systems after reconstruction. Although the distribution of cancer cells abruptly ends in one place, it may be difficult to identify this component in Figure 18 F-FDG, as sub-volume effects separate problems. Thus, extraction of 1 mm boundaries from the lower resolution technique is not expected to be successful. PET is good at detecting the presence of a tumor but may be lacking in determining precise margins. However, for radiotherapy planning, some tumor tumors need to be described. The task is to determine the most appropriate method of delimitation. The problem is illustrated in Figure 2, which shows F-FDG PET / CT images of a patient with tongue cancer. If a constant threshold technique is used to describe the tumor border, the number of tumor recurrences will vary depending on the cut-off level chosen (Figure 2B).

An equivalent way to express this is that the tumor boundary will depend on the window and the level setting selected in the delineation, which is the point that is always determined. It's not a small effect. Lesions smaller than approximately 5cm $^{18}$F appear to be more sensitive to threshold changes due to the stronger effect of partial volume effects in small tumors. In addition, separation is also possibly affected by the PET reconstruction algorithm used, filter size, and other physical parameters that are poorly controlled (6, 7).

The relative level of tumor activity and background also clearly influenced the delineation, especially at a source-to-*background* ratio of about 5 (7). These effects have been confirmed in phantoms in controlled situations (5-7). The methods by which the percentage of the maximum amount is used to determine the edge of the wound may vary from operator to operator, but it should be noted that different implementations of the quantity are "maximum". 'is in place. The maximum standardized recording value (SUV) or number in the area of interest of approximately 1 cm is usually lower than the maximum voxel (8). Because PTVs usually exceed one centimeter or more above GTV, this effect may not be as clinically large as it initially appears. The exact definition of the PET edge remains challenging.

$^{18}$F-FDG-based tumor border separation is problematic. Some attempts have been made to solve this problem and to try to implement some bearing patterns. The first study used phantoms of known size to determine standard threshold deviations of F-FDG PET voxel values that would return an appropriate object size (4). This study suggested that the threshold be set at 42% of the maximum absorption, although the study only considered values of 0.4-5.5 cm 18 to be the range where the threshold level is extremely sensitive. Another early method that showed very good accuracy in lung cancer size

The 3 definitions are intended to determine the normal activity of healthy lung tissue and its dispersion. Tumor volume was selected as the area of $^{18}$F-FDG avidity corresponding to a tumor whose absorption was more than 3 SD higher than the normal pulmonary background. This selection led to an overall good tumor definition and a good correlation of tumor size on CT and PET in untreated lung cancer (4). However, this method works best in large tumors with high absorption of $^{18}$F-FDG in areas with low background activity. Appropriate background selection and the number of background deviations can be considered tissue-specific.

In addition to these reports in the late 1990s, several studies have explored other separation methods, including the use of different thresholds, the possibility of using a set of SUVs for the threshold, the use of iterative background consideration, and the possibility of gradient detection techniques as alternative threshold contour methods. using the window and setting the level it considered most appropriate. . In any case, it makes sense to consult a nuclear medicine doctor or radiologist about tumor definition, especially since the formal training that a PET radiation oncologist has is often limited.

Examples of axial slip of a representative plane using IMRT and VMAT for an experimental arm. This example shows how the overlapping functions between the planning target volume (PTV) and the planning authority and the risk volume (PRV) are taken to determine the final PTV. There is a sharp dose gradient to maintain the urethra while maintaining an adequate dose of PTV. Competent authorities such as PTV and isodose color wash are described by legend.

***- Planning Procedures***

To guarantee a high quality of RT delivery, it is mandatory for each center to use the most current techniques, which will be assessed during initial quality assurance. All study

centers have to use intensity modulated radiotherapy (IMRT). And VMAT Radiotherapy can be performed in a LINAC system True beam Varian machine.

In general, dose description and documentation should be performed according to ICRU report 83 for MHRT and 91 for SBRT. Especially for SBRT, planning the usage of flattering filter free (FFF) approaches is recommended.

Prescription doses for the PTVs and constraints for OARs in the experimental arm for IMRT and VMAT are provided in Table 2 and Table 3 [7,17,18]. Prescription doses for the entire lung lesions must be calculated in subtraction volumes of the PTV and the Boost-PTV (PTV3). Prescription doses are the following: For PTV1 (subtraction: PTV1–PTV3): 30 Gy in 6 Gy per fraction, and for PTV2 (subtraction: PTV2–PTV3) 35 Gy in 7 Gy per fraction. The prescription dose for PTV3 ranges between 40 and 42 Gy . Initial planning should be performed with a prescription dose of 42 Gy and should be reduced up to 40 Gy in 1 Gy intervals when dose constraints are not met. In cases of large boost volumes (≥10 cc for lung lesion ), the dose to PTV3 must be restrained to 40 Gy in 8 Gy per fraction.

## 3 Discussions

The IMRT and VMAT study was designed to investigate the individualization of RT based on patient specific tumor morphology derived from CT and PET-CT for unfavorable-intermediate and lung cancer patients. For this RT dose escalation approach, one of the most promising treatment concepts was chosen: IMRT and VMAT as it enables precise delivery of ablative doses, is well tolerated and may enhance patient comfort by reducing treatment time [7,8,9].

To prove the assumption, that the postulated low α/β value of lung cancer patients [6] improves the therapeutic ratio of hypo-fractionated therapy regimes, longer follow up and more randomized data must be generated.

pCT (planning CT) -PET/CT has been shown to be highly sensitive and specific for staging of lung cancer patients and provides a markedly higher diagnostic accuracy than the current clinical standard (combination of CT and bone scans) [17]. It is unknown if better staging by pCT-PET/CT improves patient relevant outcome parameters. The IMRT and VMAT trial will therefore investigate a new and accurately staged patient cohort, leading clinical lung cancer patients' trials into the era of CT-PET/CT and challenging comparability with former trials.

A dose–response relationship for RT of primary Lung cancer has been postulated [9], but contradicting results exist whether tumor control rates are maxing out at specific doses [6,]. The significant increase in bRFS rates by focal dose escalation favors the hypothesis that the ceiling effect can be cracked [13]. The IMRT and VMAT trial will perform a boost of up to 140% and will thus provide additional information about effectiveness of focal dose escalated external beam radiotherapy (EBRT) and the biological effectiveness of hypofractionation in Lung cancer patients. Furthermore, evaluation of local failure rate and localization of local recurrences will demonstrate whether the postulated improved sensitivity and tumor coverage by inclusion of pCT-PET to ITV delineation is of clinical relevance. The correlation of dose distribution with the local recurrence pattern will provide dose–effect information. Since metastases must be confirmed preferably by pCT-PET/CT and due to the high availability of this imaging at the participating centers, this trial will give significant information about recurrence distribution patterns. The generated data of the IMRT and VMAT trial will furthermore enable the comparison of pCT alone and pCT -PET-CT for RT treatment planning, and evaluate the IGRT procedures and the safety of focal dose escalated for both techniques.

The IMRT and VMAT study is designed to examine individualization of RT based on patient-specific tumor morphology derived from pCT and PET in patients with unfavorable lung cancer patients. One of the best treatment concepts has been chosen for this focal dose escalation approach: IMRT and VMAT because it allows accurate delivery of high doses, is well tolerated and can improve patient comfort by reducing treatment time [7, 8, 9]. It should be noted that at the same time as increasing the dose to the target .

pCT-PET / CT has been shown to be highly sensitive and performance-specific in lung cancer patients and to provide higher diagnostic accuracy than the current clinical standard (combination of CT and bone scans) [11]. However, no Phase III MDGs have implemented this advanced picture as part of RT planning. It is not known whether better pCT-PET / CT performance can improve patient-related outcome parameters.

In RT in primary lung cancer patients, a dose-response relationship has been postulated [9], but there are conflicting results when the tumor control score is higher at specific doses [6]. A significant increase in the frequency of bRFS due to focal dose escalation supports the hypothesis that the ceiling effect may be impaired .The IMRT and VMAT study will increase by up to 140%, providing additional information on the efficacy of external escalating focal dose (EBRT) radiotherapy and the biological efficacy for lung cancer patients treatment. In addition, evaluation of local failure rates and localization of local recurrences will indicate whether the expected improved sensitivity and tumor coverage by including pCT-PET in our department is

of clinical significance. Correlation of dose distribution with the local recurrence pattern will provide information on the effect of the dose.

Given that metastases are best confirmed by pCT-PET / CT and due to the high availability of this image in the participating centers, this test will provide important information on recurrent resection patterns. The generated data from the IMRT and VMAT study will further allow comparison of pCT and PET-CT for RT treatment planning and evaluation of IGRT mechanisms and IMRT and VMAT safety with increased focal dose.

**Table 1**: Volumetric properties of the PTVs for the 20 Lung cancer patients

| | rimary gross tumor volume | | | | Secondary gross tumor volume | | | |
|---|---|---|---|---|---|---|---|---|
| ıbject | $V_{RIR}$ ($cm^3$) | $V_{DIR}$ ($cm^3$) | $V_{Overlap}$ ($cm^3$) | DSC | $/_{RIR}$ ($cm^3$) | $V_{DIR}$ ($cm^3$) | $V_{verlap}$ ($cm^3$) | DSC |
| 1 | **20.1** | **15.2** | **14.3** | **0.81** | **12.1** | **8.1** | **8.0** | **0.79** |
| 2 | **52.3** | **48.0** | **41.3** | **0.82** | **1.4** | **1.4** | **1.2** | **0.86** |
| 3 | **25.3** | **23.3** | **22.0** | **0.91** | **9.9** | **8.3** | **8.6** | **0.90** |
| 4 | **7.8** | **8.7** | **7.4** | **0.90** | **3.7** | **3.8** | **3.3** | **0.88** |
| 5 | **18.6** | **18.9** | **14.2** | **0.76** | **20.4** | **23.4** | **16.8** | **0.77** |
| 6 | **102.9** | **91.5** | **87.3** | **0.90** | **6.3** | **5.5** | **5.4** | **0.92** |
| 7 | **0.1** | **0.1** | **0.0** | **0.00** | **2.5** | **3.4** | **1.3** | **0.84** |
| 8 | **4.4** | **5.6** | **3.9** | **0.78** | **3.6** | **5.2** | **4.8** | **0.23** |
| 9 | **26.7** | **19.1** | **18.2** | **0.79** | **1.1** | **1.0** | **0.8** | **0.76** |
| 10 | **10.4** | **10.7** | **9.0** | **0.85** | **7.2** | **7.1** | **5.8** | **0.81** |
| 11 | **100** | **90** | **87** | **0.81** | **25** | **3.0** | **4.1** | **0.78** |
| 12 | **97** | **81** | **71** | **0.79** | **23** | **4.1** | **2.3** | **0.82** |
| 13 | **45** | **47** | **25** | **0.91** | **18** | **8.2** | **4.3** | **0.8** |
| 14 | **26** | **22** | **17** | **0.87** | **17** | **11** | **3.5** | **0.9** |
| 15 | **74** | **68** | **50** | **0.74** | **22** | **8** | **5.2** | **0.84** |
| 16 | **63** | **71** | **47** | **0.72** | **32** | **7.6** | **3.9** | **0.82** |
| 17 | **41** | **31** | **28** | **0.84** | **18** | **10.3** | **4.1** | **0.76** |
| 18 | **120** | **115** | **76** | **0.92** | **21** | **9.3** | **2.3** | **0.72** |
| 19 | **123** | **104** | **89** | **0.87** | **22** | **8.1** | **3.8** | **0.83** |
| 20 | **111** | **98** | **70** | **0.82** | **19** | **12** | **4.1** | **0.86** |

The volumes corresponding to the GTVs drawn using the rigid and deformable image registration are labeled as VRIR and VDIR, respectively.

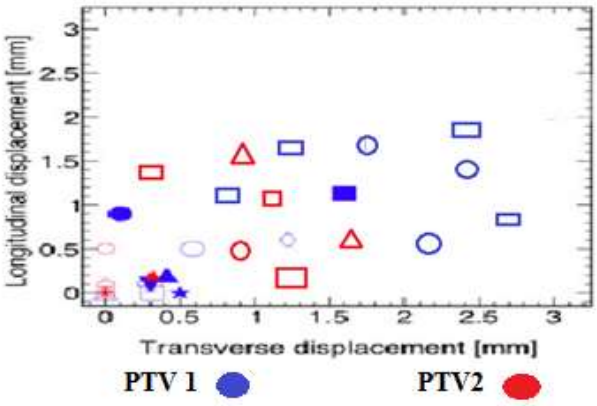


**Comparing the position of PTVs defined using RIR and DIR PET images.** The displacement along the z-axis is shown as a function of the displacement in the transverse plane for the lung cancer subjects. One-point falls beyond the range of the histogram for a lung subject, where displacements of 2.8 mm in the transverse plane and 1.75 mm along the longitudinal axis are observed. Twenty different symbols are used for the 20 different subjects.

**Table 2**: Percentage of the volume of the PTVs receiving at least 100% of the prescribed dose.

| | Lung patients | | | |
|---|---|---|---|---|
| Patient | **Primary node** | | **Secondary node** | |
| No | | | | |
| | **% $V_{RIR}$** | **% $V_{DIR}$** | **% $V_{RIR}$** | **% $V_{DIR}$** |
| 1 | **94** | **95** | **97** | **96** |
| 2 | **98** | **99** | **96** | **97** |
| 3 | **100** | **100** | **100** | **100** |
| 4 | **100** | **100** | **98** | **100** |
| 5 | **100** | **100** | **91** | **91** |
| 6 | **97** | **97** | **100** | **100** |
| 7 | **100** | **100** | **98** | **95** |
| 8 | **89** | **94** | **97** | **98** |
| 9 | **100** | **100** | **97** | **96.3** |
| 10 | **67** | **96** | **95** | **97.4** |
| 11 | **120** | **98.2** | **96.3** | **100** |
| 12 | **100** | **96.5** | **97** | **96** |

| | | | | |
|---|---|---|---|---|
| 13 | **78** | **97.1** | **96** | **96.1** |
| 14 | **96** | **96.3** | **95** | **98** |
| 15 | **97** | **97.1** | **97** | **100** |
| 16 | **97** | **95.3** | **96** | **95.7** |
| 17 | **98** | **97.23** | **97** | **96.2** |
| 18 | **100** | **97.6** | **96** | **97.5** |
| 19 | **98** | **98.4** | **97** | **96.2** |
| 20 | **97** | **96.4** | **95.7** | **96.3** |

The convention described in Table 1 is used.

**Lung cancer analysis**

Twenty patients with lung cancer were selected for this study. The properties of GTV are shown in Table 3. Five subjects had secondary tumor volumes in the mediastinum or hilar region identified by PET images and contoured. The size of the GTV ranges from about 3 $cm^3$ to more than 350 $cm^3$. The spatial difference between the center of gravity of GTV from RIR and DIR was found to be consistently small in all patients, averaging 0.6 mm with a standard deviation of 0.6 mm. These numbers increased to 0.7 mm when lymphatic secondary nodes were excluded. In all 20 patients with multiple contour nodes, GTV observed the same transitions along the longitudinal axis, while transitions in the transverse plane were different. The mean cube agreement coefficient was 0.93 (95% confidence interval: 0.80–1.00) and 0.90 when lymph nodes were excluded. All PTVs received at least 95% of the prescribed dose up to ≥ 99% of their volume, except for the secondary GTV in three patients 10,13,15, where a lower dose was administered to the mediastinum to preserve the heart and lungs.

**Table 3: Volumetric properties of the GTVs for the 20 lung cancer Patients.**

| | Primary gross tumor volume | | | | Secondary gross tumor volume | | | |
|---|---|---|---|---|---|---|---|---|
| Patient No. | **V RIR ($cm^3$)** | **V DIR ($cm^3$)** | **V Overlap ($cm^3$)** | **DSC** | **V RIR ($cm^3$)** | **V DIR ($cm^3$)** | **V Overlap ($cm^3$)** | **DSC** |
| 1 | **39.3** | **37.2** | **34.3** | **0.90** | **36** | **18** | **12** | **na** |
| 2 | **71.4** | **77.2** | **65.5** | **0.88** | **61** | **58** | **2.8** | **na** |
| 3 | **14.4** | **14.5** | **13.0** | **0.90** | **2.7** | **2.9** | **2.7** | **0.96** |
| 4 | **13.8** | **14.5** | **12.6** | **0.89** | **18** | **16.5** | **15.6** | **0.98** |
| 5 | **11.4** | **11.0** | **10.5** | **0.94** | **6.8** | **6.8** | **6.8** | **1.00** |
| 6 | **38.0** | **36.2** | **28.1** | **0.76** | **27.0** | **27.0** | **27.0** | **1.00** |
| 7 | **26.4** | **26.4** | **24.0** | **0.91** | **21** | **18** | **17** | **0.95** |
| 8 | **356.8** | **356.5** | **330.8** | **0.93** | **23** | **25** | **18** | **na** |
| 9 | **61.1** | **59.8** | **55.4** | **0.92** | **12.6** | **12.6** | **12.6** | **1.00** |
| 10 | **63.3** | **62.7** | **60.9** | **0.97** | **21.0** | **21.0** | **21.0** | **1.00** |
| 11 | **57.3** | **56** | **54** | **0.97** | **18** | **31** | **32** | **1.00** |
| 12 | **45.6** | **44** | **42.3** | **0.85** | **24** | **32.5** | **24** | **0.98** |
| 13 | **71** | **68** | **63** | **0.92** | **27** | **28.6** | **28** | **0.99** |
| 14 | **62** | **60** | **57** | **0.92** | **45** | **22.7** | **45** | **0.96** |
| 15 | **45** | **41** | **40** | **0.93** | **28** | **21.7** | **17** | **0.97** |
| 16 | **86** | **83** | **80** | **0.88** | **15** | **28.3** | **18** | **1.00** |
| 17 | **24** | **21** | **20** | **0.91** | **13.8** | **18.9** | **16** | **0.97** |
| 18 | **58** | **52** | **51.3** | **0.92** | **14.2** | **27.8** | **13.8** | **0.95** |
| 19 | **81** | **76** | **70** | **0.86** | **18.3** | **31** | **12.7** | **0.96** |
| 20 | **96** | **86** | **83** | **0.85** | **22** | **22** | **12.8** | **0.97** |

-The convention described in Table 1 is used. The difference in the average radiation dose received by the PTVs drawn from the RIR and DIR was less than 1% for all subjects. The differences in V100% between RIR and DIR were typically small and at most 5% as shown in Table 2

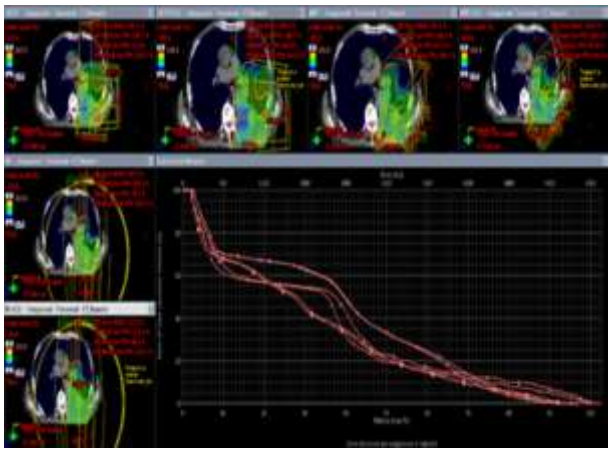

Several studies have been conducted to examine the performance and usefulness of DIR. Schwartz et al. [10] performed DIRs between planning CT and other CT scans obtained during irradiation in 22 head and neck cancer patients to evaluate different approaches to adaptive radiotherapy. They show that the process of adaptive radiation therapy is possible with the use of DIR and that the healing of endangered organs can be achieved. Castadot et al. [11], Fallone et al. [12] Zhong et al. [13] developed several phantom measures to evaluate the biased registration package and came up with a protocol for systematic DIR evaluation. Senthi et al. [14] reported differences in RIR and DIR in 10 re-irradiated lung cancer patients who underwent initial CT scans using a follow-up CT scheme used in the second treatment plan. They observed improvements in the registration of risk authorities when using DIR as opposed to RIR; however, they did not investigate possible changes in the patient's dosimetry. Similarly, Ireland et al. [15] estimated differences in RIR and DIR in five head and neck cancer patients with PET / CT scans compared to scheduled CT scans. They observed that DIR provides a more accurate registration than RIR for a set of anatomical landmarks, but did not evaluate differences in patient dosimetry. Yin and others. [16] examined several DIR packages to accurately record normal tissue function (SPECT) in CT planning. Despite these publications, no studies have yet been conducted to examine possible differences in the definition of total gross tumor volume (GTV) and possible changes in GTV doses, whether RIR or DIR are used. between PET / CT and CT scan planning.

There were consistent longitudinal differences in GTV placement with contoured RIRs and DIRs among all subjects with multiple tumors. The internal RIR within the DIR algorithm can cause constant variations in longitudinal location. This observation also indicates that DIR was performed on a point-by-cut basis, i.e., no longitudinal deformations were performed. Although the GTV size differs by 30% between RIR and DIR, their placement is the same within 2.8 mm and the cube matching coefficients are high for 32 of the 33 tumor volumes, indicating a high level of fitness. In lung cancer subjects, the location and size of mediastinal and hilar GTVs were observed to be similar in 4 of 5 patients because radiation oncologists chose to treat volume not limited to FDG. -avid node (s), but also includes adjacent lymph nodes suspected of being affected. In these cases, GTVs were designed based on the anatomy of the patient with scheduled and diagnostic CT scans.

Clinical target volumes were performed around an RIR-defined GTV with 5-8 mm margins for the head and neck and 7 mm for lung cancer patients. In addition, 4 mm margins have been added to create volume targeting (PTV) plans. External tree planning was done immediately using RIR-defined PTV. The radiation dose delivered by RIR and DIR-drawn GTVs is therefore very similar in that DIR-defined GTVs are in RIR-defined PTVs.The survival of healthy tissues and organs at risk has not been evaluated due to the small changes observed in the position between RIR-defined and DIR-defined GTV. The potential profit is assumed to be small.

**Limitations: -**

It should be noted that when DIR is applied to PET images, voxel intensity (Bq / ml) cannot be maintained. It was judged to affect the highest standardized record value of less than 1% and was considered to have no value in determining GTV compared to random systematic manual uncertainties that proved to be significant [18].Although lung tumors are located in the upper lung area, where sensitivity to respiratory movements is reduced, gating techniques significantly reduce sensitivity to respiratory movements during the acquisition of planning CT and PET / CT. The large time lag between obtaining a scheduled CT and a PET / CT scan of 1-15 days may be a major factor in the apparent tumor progression, especially in fast-growing patients. Finally, the separation of hilar and mediastinal nodes by radiation oncologists in lung cancer patients is often based on anatomy rather than metabolic data, which may be the result. As such, data are presented for patients with lung cancer and these patients do not have secondary nodes.

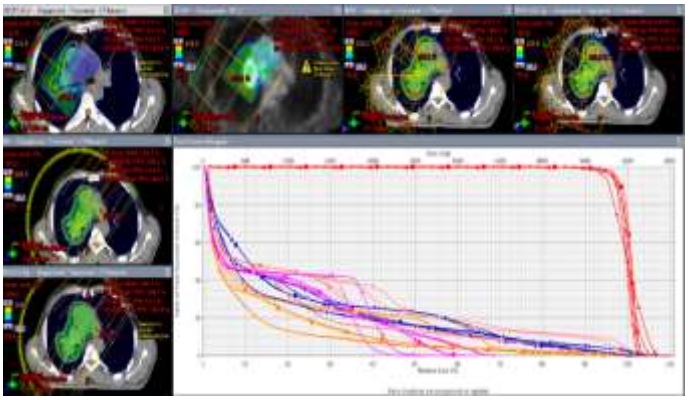

## 4 Conclusions

- Radiation therapy plays an important role in cancer treatment management. The primary goal of radiotherapy is to achieve improved local control with increasing tumor dose while reducing the possibility of side effects by reducing the radiation exposure of healthy surrounding organs. Good delineation is required for a good definition of gross tumor volume to avoid inadequate treatment.
- CT-based RTP contains only anatomical information that is not sufficient for this aspect, so advanced imaging techniques have become critical. PET / CT is used for this purpose primarily as one of the medical images combining metabolic and anatomical functions. PET / CT is a recognized modality for diagnosing, staging, and evaluating tumor response in various types of cancer.
- There are increasing data comparing the use of PET / CT with other imaging techniques for RTP, and there are disputes about the appropriate use of PET / CT. Finally, the evaluation of PET / CT images is useful for accurate

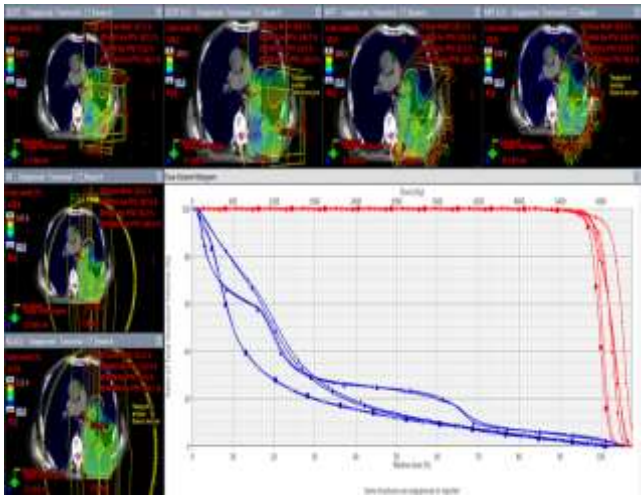

definition and is also an additional method for determining the target volume of radiotherapy. Using PET / CT information with Velocity AI features such as software joint image registration, threshold segmentation, and response evaluation, it can be practical in planning and monitoring radiotherapy.

- Distorted image recording has become an important part of image-driven protocols and adaptive radiotherapy. Commercial software for performing DIR is now available at the BC Cancer Agency for recording PET / CT images for CT scan planning, but this study does not show much benefit. If there are no significant anatomical differences between PET / CT and Scheduled CT, the skewed registration value between PET / CT and Scheduled CT scans are indicated as a marginal value when adjusting gross tumor volumes.

**Abbreviations**

CT: Computed Tomography; PET: Positron Emission Tomography; FDG: Fluorodeoxyglucose; RIR: Rigid image registration; DIR: Deformable image registration; GTV: Gross tumor volume; IMRT: Intensity modulated radiotherapy; DSC: Dice similarity coefficient; SUV: Standardized Uptake Value; PTV: Primary target volume.

## References

[1] Visioni A, Kim J. Positron emission tomography for benign and malignant disease. Surg Clin North Am. 2011; 91:249–266.

[2] Price PM, Green MM. Positron emission tomography imaging approaches for external beam radiation therapies: current status and future developments. Br J Radiol. 2011;84 Spec No 1:S19–S34.

[3] Cuaron J, Dunphy M, Rimner A. Role of FDG-PET scans in staging, response assessment, and follow-up care for non-small cell lung cancer. Front Oncol. 2012; 2:208.

[4] Newbold K, Powell C. PET/CT in radiotherapy planning for head and neck cancer. Front Oncol. 2012; 2:189.

[5] International Atomic Energy Agency. The Role of PET/CT in radiation treatment planning for cancer patient treatment: IAEA-TECDOC-1603. Vienna: IAEA; 2008. Role of PET in radiation therapy planning for specific tumor types; pp. 7–21.

[6] Wahl RL, Jacene H, Kasamon Y, Lodge MA. From RECIST to PERCIST: evolving considerations for PET response criteria in solid tumors. J Nucl Med. 2009;50(Suppl 1):122S–150S.

[7] Hwang AB, Bacharach SL, Yom SS, Weinberg VK, Quivey JM, Franc BL, Xia P. Can positron emission tomography (PET) or PET/Computed Tomography (CT) acquired in a nontreatment position be accurately registered to a head-and-neck radiotherapy planning CT? Int J Radiat Oncol Biol Phys. 2009; 73:578–584.

[8] Caldwell CB, Mah K, Basran PS. Evaluation of a combined positron emission tomography (PET)/computed tomography (CT) scanner for radiation therapy simulation. Radiother Oncol. 2004;72: S60–S60.

[9] Brock KK. Image registration in intensity-modulated, image-guided and stereotactic body radiation therapy. Front Radiat Ther Oncol. 2007; 40:94–115.

[10] Schwartz DL, Garden AS, Shah SJ, Chronowski G, Sejpal S, Rosenthal DI, Chen Y, Zhang Y, Zhang L, Wong P-F, Garcia JA, Kian Ang K, Dong L. Adaptive radiotherapy for head and neck cancer–dosimetric results from a prospective clinical trial. Radiother Oncol. 2013; 106:80–84.

[11] Castadot P, Lee JA, Parraga A, Geets X, Macq B, Grégoire V. Comparison of 12 deformable registration strategies in adaptive radiation therapy for the treatment of head and neck tumors. Radiother Oncol. 2008;89:1–12. doi: 10.1016/j.radonc.2008.04.010.

[12] Fallone BG, Rivest DRC, Riauka TA, Murtha AD. Assessment of a commercially available automatic deformable registration system. J Appl Clin Med Phys. 2010; 11:3175.

[13] Zhong H, Kim J, Chetty IJ. Analysis of deformable image registration accuracy using computational modeling. Med Phys. 2010;37:970–979.

[14] Senthi S, Griffioen GHMJ, van Sörnsen de Koste J, Slotman BJ, Senan S. Comparing rigid and deformable dose registration for high dose thoracic re-irradiation. Radiother Oncol. 2013; 106:323–326.

[15] Ireland RH, Dyker KE, Barber DC, Wood SM, Hanney MB, Tindale WB, Woodhouse N, Hoggard N, Conway J, Robinson MH. Nonrigid image registration for head and neck cancer radiotherapy treatment planning with PET/CT. Int J Radiat Oncol Biol Phys. 2007; 68:952–957.

[16] Yin LS, Tang L, Hamarneh G, Gill B, Celler A, Shcherbinin S, Fua TF, Thompson A, Liu M, Duzenli C, Sheehan F, Moiseenko V. Complexity and accuracy of image registration methods in SPECT-guided radiation therapy. Phys Med Biol. 2010; 55:237–246.

[17] Basran PS, Capaldi D. On Quantitative assessment of deformable CT-CT registration. Proceedings of the Joint Scientific Meeting of CARO-COMP 2013. 2013. p. 8

[18] Hatt M, Cheze-Le Rest C, Aboagye EO, Kenny LM, Rosso L, Turkheimer FE, Albarghach NM, Metges J-P, Pradier O, Visvikis D. Reproducibility of 18F-FDG and 3'-deoxy-3'-18F-fluorothymidine PET tumor volume measurements. J Nucl Med. 2010;51:1368–1376.